Photophoresis of an Aerosol Sphere in a Spherical Cavity

Huan J. Keh*

Department of Chemical Engineering, National Taiwan University,
Taipei 106-17, Taiwan ROC

This study examines the quasisteady photophoretic motion of a spherical aerosol particle with arbitrary thermal conductivity and surface properties, located at the center of a spherical cavity and exposed to a radiative flux. Assuming a small Knudsen number, the fluid flow is described by a continuum model with a temperature jump, thermal creep, and frictional slip on the solid surfaces. In the limit of the small Peclet and Reynolds numbers, appropriate equations of conservation of energy and momentum are solved for the system and the photophoretic velocity of the particle is obtained in closed form. The normalized photophoretic mobility increases with the relative conductivity of the particle. The boundary effect of the cavity wall on the photophoresis of an aerosol particle is generally quite significant in appropriate situations. In practical aerosol systems, the boundary effect on photophoresis is much weaker than on gravitational field driven motion.

Keywords: photophoresis, aerosol sphere, boundary effect.

1. Introduction

A small particle, when suspended in a gaseous medium and exposed to an intense light beam, migrates parallel to the direction of the light. This phenomenon, a direct result of the uneven heating of the light absorbing particle (and therefore, its adjacent gas molecules), was termed photophoresis by its discoverer, Ehrenhaft, around 1910 [1, 2]. The photophoretic (or thermophoretic) effect can be partly explained by using the kinetic theory of gases [3]. The higher-energy molecules in the hot region of the gas impinge on the particle with greater momentum than molecules from the cold region, thus causing the particle to migrate in the direction opposite to the surface temperature gradient. The photophoretic force on an aerosol particle can thus be directed either toward (negative photophoresis) or away from (positive photophoresis) the light source, depending on the optical characteristics of the particle. If the particle is opaque and the incident light energy is absorbed and dissipated directly on its front surface, positive photophoresis results. Conversely, if the light beam is partially transmitted and focused internally (e.g. the rear surface), the direction of the motion may differ.

Photophoresis has been observed for numerous particulate materials in the diameter range between 10^{-8} and 10^{-3} m, and at pressures from above 1 atm to below 1 torr, under illumination intensities comparable with sunlight [2]. Consequently, photophoresis investigations are relevant to various fields, including cloud physics, aerosol science, and environmental engineering. For example, measurements of the photophoretic force or the reversal point from positive to negative

*Corresponding author:
Tel.: +886-2-23635462
Fax: +886-2-23623040.
E-mail address: huan@ccms.ntu.edu.tw.

photophoresis as the photophoretic spectroscopy is elaborated can be used to determine the physical properties (e.g. the complex refractive index) and chemical composition of aerosol particles [4]. The photophoretic phenomena of aerosol particles subjected to coherent light beams have been applied to the development of laser atmospheric monitoring methods [5]. This endeavor found that, because of the effect of both positive and negative photophoresis, stratospheric aerosol particles may rise against gravity while others fall considerably more rapidly than they would under gravity alone [6]. Considering that radiative transfer can account for approximately 95% of the total heat flux in pulverized-coal furnaces, the driving force for photophoresis of small particles in combustion environments can be significantly greater than that for thermophoresis [7].

Assuming a small Knudsen number (l/a, where a denotes the radius of the particle and l represents the mean free path of the surrounding gas molecules), a small Reynolds number, and a small Peclet number, as well as allowing for the effects of temperature jump, thermal slip, and hydrodynamic slip at the gas-particle interface, Reed [8] and Mackowski [7] obtained the photophoretic velocity of an aerosol sphere illuminated by an intense light beam as

$$U^{(0)} = -\frac{2C_s J_1 \eta I}{3(1+2C_m l/a)(2k+k_p+2k_p C_t l/a)\rho T_0}. \quad (1)$$

Here, I denotes the intensity of the incident light (incoming illumination energy flux); ρ, η, and k represent the density, viscosity, and thermal conductivity of the gas, respectively; k_p is the thermal conductivity of the particle; T_0 denotes the absolute temperature of the bulk gas; J_1 represents the so-called photophoretic asymmetry factor [9] defined by Eq. (26), which can be either positive (negative photophoresis) or negative (positive photophoresis); and C_s, C_t, and C_m are dimensionless coefficients accounting for the thermal slip, temperature jump, and frictional slip phenomena, respectively, at the particle surface, and must be determined experimentally for each gas-solid system. A set of reasonable kinetic-theory values for complete thermal and momentum accommodations appears to be C_s =1.17, C_t =2.18, and C_m =1.14 [10]. The extension of Eq. (1) to the photophoretic velocity of a circular cylindrical particle normal to its axis has recently been derived [11].

In numerous applications of photophoresis, aerosol particles are not isolated and will move in the presence of neighboring particles and/or boundaries. For example, the mechanism and rate of deposition of photophoretic particles on surfaces are of practical interest. Consequently, examining the behavior of a particle under photophoretic forces when in the proximity of rigid boundaries is relatively important. However, the boundary effects on the photophoretic motion of aerosol particles remain unexplored. This work aims to obtain insights into the boundary effects on the photophoresis of an aerosol particle inside a small pore. This type of problem is difficult to solve because of the complexity of actual system geometry. To overcome the mathematical complexities involved in the problem of a sphere in a cylinder (which is a widely used model for particles in pores), the photophoresis of a spherical particle situated at the center of a spherical cavity is examined. Although the geometry of the spherical cavity is an idealized abstraction of a real system, the analytical results obtained for this geometry agree closely with available expressions for boundary effects on the partition coefficient [12, 13], settling velocity [14, 15], and electrophoretic mobility [16, 17] of a spherical particle in a cylindrical pore. The spherical symmetry in this model system allows a precise analytical solution to be obtained, and the analytical results demonstrate that the boundary effects on the photophoresis of an aerosol particle can be significant in most situations.

2. Analysis

This section considers the quasisteady photophoretic motion of a spherical particle with radius a and arbitrary thermal conductivity and surface properties in a concentric spherical cavity (or pore) with radius b filled with a gaseous medium, as illustrated in Fig. 1. An incident light is imposed on the particle in the z direction with intensity I and the photophoretic velocity of the particle is $U\mathbf{e}_z$, where $\mathbf{e}_z$ denotes the unit vector in the positive z direction. The Knudsen numbers l/a and $l/(b-a)$ are assumed to be sufficiently small that the fluid flow is in the continuum regime and the Knudsen layers adjacent to the solid surfaces are not overlapping. The fluid is allowed to slip, both thermally and frictionally, and the temperature may jump on the solid surfaces. The origin of the spherical coordinate system (r,θ,ϕ) is set at the center of the particle. This investigation aims to determine the correction to Eq. (1) for the particle owing to the presence of the cavity.

The Peclet number of this axisymmetric problem is assumed to be small. Consequently, the equation of energy governing the temperature distribution $T(r,\theta)$ for the fluid of constant thermal conductivity k is the Laplace equation,

$$\nabla^2 T = 0 \qquad (a \le r \le b). \tag{2}$$

The temperature distribution $T_\mathrm{p}(r,\theta)$ inside the radiation-absorbing particle is described by

$$\nabla^2 T_\mathrm{p} = -\frac{1}{k_\mathrm{p}} Q(r,\theta) \qquad (r \le a), \tag{3}$$

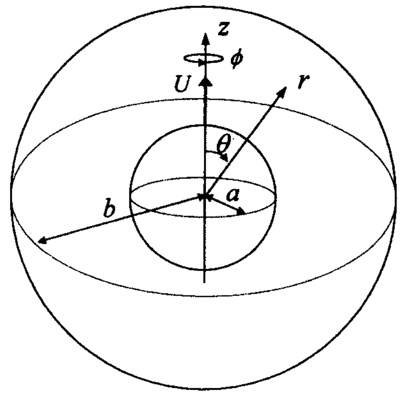

Fig. 1 . Geometrical sketch for the photophoretic motion of a spherical particle in a concentric spherical cavity.

where k_p denotes the thermal conductivity of the particle and $Q(r,\theta)$ denotes the volumetric thermal energy generation rate resulting from local radiation absorption. For a plane monochromatic wave, the source function $Q(r,\theta)$ is related to the electric field $\mathbf{E}(r,\theta)$ inside the particle according to the theory of Lorenz-Mie [7, 18],

$$Q(r,\theta) = \frac{4\pi \upsilon \kappa I}{\lambda_0} \frac{|\mathbf{E}(r,\theta)|^2}{|\mathbf{E}_0|^2} = \frac{4\pi \upsilon \kappa I}{\lambda_0} B(\zeta,\theta). \tag{4}$$

Here, υ and κ denote the real and imaginary parts of the complex refractive index N ($N = \upsilon + i\kappa$) of the particle, $\mathbf{E}_0$ represents the incident electric field strength, λ_0 is the wavelength of the incident radiation, $B(\zeta,\theta)$ denotes the dimensionless electric field distribution function, and $\zeta = r/a$.

The boundary conditions at the particle surface ($r = a$) require that the normal heat fluxes be continuous and a temperature jump occur which is proportional to the normal temperature gradient [3]. Furthermore, the fluid temperature at the cavity wall approaches the bulk-gas temperature T_0 which is a constant. Thus,

$$r = a: \quad k\frac{\partial T}{\partial r} = k_{\rm p}\frac{\partial T_{\rm p}}{\partial r}, \tag{5a}$$

$$T - T_{\rm p} = C_{\rm t} l \frac{\partial T}{\partial r}, \tag{5b}$$

$$r = 0: \quad T_{\rm p} \text{ is finite,} \tag{6}$$

$$r = b: \quad T = T_0, \tag{7}$$

where $C_{\rm t}$ is the temperature jump coefficient about the particle surface.

A sufficiently general solution to Eqs. (2) and (3) is

$$T = T_0 + \frac{aI}{k}\sum_{n=0}^{\infty} A_n[\zeta^{-n-1} - \lambda^{2n+1}\zeta^n]P_n(\cos\theta), \tag{8}$$

$$T_{\rm p} = T_0 + \frac{aI}{k_{\rm p}}\sum_{n=0}^{\infty}[B_n\zeta^n + S_n(\zeta)]P_n(\cos\theta), \tag{9}$$

where

$$S_n(\zeta) = \frac{2\pi\upsilon\kappa a}{\lambda_0}[\zeta^n \int_\zeta^1 t^{-n+1}\int_0^\pi B(t,\theta)P_n(\cos\theta)\sin\theta\, d\theta\, dt$$
$$+\zeta^{-n-1}\int_0^\zeta t^{n+2}\int_0^\pi B(t,\theta)P_n(\cos\theta)\sin\theta\, d\theta\, dt], \tag{10}$$

P_n denotes the Legendre polynomial of order n, and $\lambda = a/b$. A solution of this form immediately satisfies boundary conditions (6) and (7), and the unknown coefficients A_n and B_n are determined using the boundary conditions at the particle surface.

Applying boundary conditions (5a) and (5b) on the surface of the particle to Eqs. (8) and (9) obtains the following:

$$A_n = \frac{nS_n(1) - S_n'(1)}{nk^* + (n+1)(1+nk^*C_{\rm t}^*) + n(1-k^*+k^*C_{\rm t}^*)\lambda^{2n+1}}, \tag{11}$$

$$B_n = -\frac{S_n(1)(n\lambda^{2n+1}+n+1) + k^*S_n'(1)[1-\lambda^{2n+1}+C_{\rm t}^*(n\lambda^{2n+1}+n+1)]}{nk^* + (n+1)(1+nk^*C_{\rm t}^*) + n(1-k^*+k^*C_{\rm t}^*)\lambda^{2n+1}}, \tag{12}$$

where

$$k^* = k_{\rm p}/k, \tag{13a}$$

$$C_{\rm t}^* = C_{\rm t} l/a, \tag{13b}$$

and the prime on $S_n(\zeta)$ means differentiation with respect to ζ. Notably the dimensionless parameter $k^*C_{\rm t}^*$ denotes the relative resistance caused by the temperature jump on the particle surface with respect to heat conduction inside the particle.

With knowledge of the solution for temperature distribution, the flow field can now be found. The fluid surrounding the particle is assumed to be incompressible and Newtonian. Meanwhile, owing to the low Reynolds number, the fluid motion caused by the photophoretic migration of the particle is governed by the quasisteady fourth-order differential equation for axisymmetric creeping flows,

$$E^4\Psi = E^2(E^2\Psi) = 0, \tag{14}$$

where $\Psi(r,\theta)$ is the Stokes stream function. In spherical coordinates, the Stokesian operator E^2 is given by

$$E^2 = \frac{\partial^2}{\partial r^2} + \frac{\sin\theta}{r^2}\frac{\partial}{\partial\theta}\left(\frac{1}{\sin\theta}\frac{\partial}{\partial\theta}\right). \tag{15}$$

The stream function Ψ is related to the r and θ components of the velocity field by

$$v_r = -\frac{1}{r^2\sin\theta}\frac{\partial\Psi}{\partial\theta}, \tag{16a}$$

$$v_\theta = \frac{1}{r\sin\theta}\frac{\partial\Psi}{\partial r}. \tag{16b}$$

Owing to the thermal and frictional slip velocities along the solid-fluid interface, the boundary conditions for the fluid velocity on the particle surface are [19]

$$r = a: \quad v_r = U\cos\theta, \tag{17a}$$

$$v_\theta = -U\sin\theta + \frac{C_{\rm m}l}{\eta}\tau_{r\theta} + \frac{C_{\rm s}\eta}{\rho T_0}\frac{\partial T}{\partial\theta}. \tag{17b}$$

Here, $C_{\rm m}$ and $C_{\rm s}$ are the frictional and thermal slip coefficients, respectively, around the surface of the particle, while $\tau_{r\theta}$ represents the shear stress for the fluid flow,

$$\tau_{r\theta} = \eta\left[r\frac{\partial}{\partial r}\left(\frac{v_\theta}{r}\right) + \frac{1}{r}\frac{\partial v_r}{\partial\theta}\right], \tag{18}$$

and U denotes the photophoretic velocity of the particle to be determined. The derivative $\partial T/\partial\theta$ along the particle surface can be evaluated using the temperature distribution given by Eq. (8). The validity of the expression for the thermal slip velocity in Eq. (17b) is based on the assumption that the fluid temperature is only slightly nonuniform on the length scale of the particle radius. Notably, the slip-flow boundary condition is not only applicable in the continuum regime ($l/a << 1$), but also appears valid even for some cases in the molecular flow regime ($l/a \geq 1$). Generally, the slip condition becomes increasingly important for small particles. Meanwhile, at the isothermal cavity wall, the boundary conditions for the fluid are

$$r = b: \quad v_r = 0, \tag{19a}$$

$$v_\theta = -\frac{\hat{C}_m l}{\eta} \tau_{r\theta}, \tag{19b}$$

where $\hat{C}_m$ denotes the frictional slip coefficient around the surface of the wall.

A solution to Eq. (14) suitable for satisfying boundary conditions on the spherical surfaces is [15]

$$\Psi = (Cr^{-1} + Dr + Er^2 + Fr^4)\sin^2\theta, \tag{20}$$

where the constants C, D, E, and F are determined based on Eqs. (8), (16), (17) and (19). The procedure is straightforward, with the result

$$C = a^3\omega\{2[(1+3\hat{C}_m^*) - (1-3C_m^*)\lambda^3]U + 3A_1[2(1+3\hat{C}_m^*) - 3(1+2\hat{C}_m^*)\lambda + \lambda^3]V\}, \tag{21a}$$

$$D = -3a\omega\{2[(1+2C_m^*)(1+3\hat{C}_m^*) - (1-3C_m^*)(1-2\hat{C}_m^*)\lambda^5]U + A_1[2(1+3\hat{C}_m^*) - 5\lambda^3 + 3(1-2\hat{C}_m^*)\lambda^5]V\}, \tag{21b}$$

$$E = \omega\{[9(1+2C_m^*)(1+2\hat{C}_m^*)\lambda - 5\lambda^3 - 4(1-3C_m^*)(1-3\hat{C}_m^*)\lambda^6]U + 3A_1[3(1+2\hat{C}_m^*)\lambda - 5\lambda^3 + 2(1-3\hat{C}_m^*)\lambda^6]V\}, \tag{21c}$$

$$F = -3a^{-2}\omega\{[(1+2C_m^*)\lambda^3 - (1-2\hat{C}_m^*)\lambda^5]U + A_1[\lambda^3 - 3(1-2\hat{C}_m^*)\lambda^5 + 2(1-3\hat{C}_m^*)\lambda^6]V\}, \tag{21d}$$

where

$$C_m^* = C_m l / a, \tag{22a}$$

$$\hat{C}_m^* = \hat{C}_m l / a, \tag{22b}$$

$$V = \frac{2C_s \eta I}{3k\rho T_0}(1-\lambda^3), \tag{23}$$

which is a characteristic migration velocity of the particle, and

$$\omega = [8(1+3C_m^*)(1+3\hat{C}_m^*) - 18(1+2C_m^*)(1+2\hat{C}_m^*)\lambda + 20\lambda^3 - 18(1-2C_m^*)(1-2\hat{C}_m^*)\lambda^5 + 8(1-3C_m^*)(1-3\hat{C}_m^*)\lambda^6]^{-1}. \tag{24}$$

Based on the above solution, the components of the fluid velocity in this axisymmetric flow (with $v_\phi = 0$) can be calculated using Eq. (16).

The coefficient A_1 in Eq. (21) can be calculated using the definition of Eq. (11),

$$A_1 = \frac{J_1}{2 + k^* + 2k^*C_t^* + (1 - k^* + k^*C_t^*)\lambda^3}, \tag{25}$$

where J_1 denotes the so-called photophoretic asymmetry factor,

$$J_1 = \frac{6\pi\upsilon\kappa a}{\lambda_0}\int_0^1\int_0^\pi B(\zeta,\theta)\zeta^3\cos\theta\sin\theta\, d\theta\, d\zeta, \tag{26}$$

which depends on the complex refractive index ($N = \upsilon + i\kappa$) and the normalized size ($2\pi a/\lambda_0$) of the particle. The asymmetry factor represents a weighted integration of the heat source function over the particle volume and defines the sign and magnitude of the photophoretic force. If $J_1 < 0$, the particle moves towards the light beam (positive photophoresis), while if $J_1 > 0$, the particle moves away from the light beam (negative photophoresis). For a completely opaque spherical particle the heat sources are concentrated on the illuminated part of the particle surface, namely,

$$B(\zeta,\theta) = \begin{cases} \dfrac{-\lambda}{2\pi\upsilon\kappa a}\cos\theta\,\delta(\zeta-1) & \text{for } \dfrac{\pi}{2} \leq \theta \leq \pi \\ 0 & 0 \leq \theta \leq \dfrac{\pi}{2}, \end{cases} \tag{27}$$

where $\delta(\zeta - 1)$ is a Dirac delta function which equals infinity if $\zeta = 1$ and vanishes otherwise. Substituting Eq. (27) into Eq. (26) results in $J_1 = -1/2$ given that

$$\int_0^1 g(\zeta)\delta(\zeta-1)d\zeta = (1/2)g(1).$$

Obviously, the range of the asymmetry factor is $-1/2 \leq J_1 \leq 1/2$. According to Eq. (1), the photophoretic velocity at illumination of an intensity comparable with the solar constant ($1{,}353\ \mathrm{W\,m^{-2}}$) is of the order of 10^{-5} $\mathrm{m\,s^{-1}}$.

The drag force (in the z direction) exerted by the fluid on the particle is [15]

$$F_\mathrm{d} = 8\pi\eta D \tag{28}$$

Because the particle is freely suspended in the fluid, the net force exerted by the fluid on the particle must vanish; viz., $D = 0$. Given this constraint, Eq. (21b) yields the photophoretic velocity of the particle,

$$U = -A[2(1+3\hat{C}_\mathrm{m}^*) - 5\lambda^3 + 3(1-2\hat{C}_\mathrm{m}^*)\lambda^5] \\ [2(1+2C_\mathrm{m}^*)(1+3\hat{C}_\mathrm{m}^*) - 2(1-3C_\mathrm{m}^*)(1-2\hat{C}_\mathrm{m}^*)\lambda^5]^{-1} V. \tag{29}$$

This result is generated from the combined effects of particle-cavity interactions on the temperature and fluid velocity fields.

3. Results and Discussion

The analytical solutions of the temperature and flow fields in the sphere-in-cavity system and of the photophoretic velocity of the particle have been obtained above. This migration velocity can be expressed as

$$U = U^{(0)}(1-\lambda^3)(1+G\lambda^3)^{-1}(1+2C_\mathrm{m}^*)[2(1+3\hat{C}_\mathrm{m}^*) - 5\lambda^3 + 3(1-2\hat{C}_\mathrm{m}^*)\lambda^5] \\ [2(1+2C_\mathrm{m}^*)(1+3\hat{C}_\mathrm{m}^*) - 2(1-3C_\mathrm{m}^*)(1-2\hat{C}_\mathrm{m}^*)\lambda^5]^{-1}, \tag{30}$$

where

$$U^{(0)} = -\frac{2C_\mathrm{s} J_1 \eta I}{3(1+2C_\mathrm{m}^*)(2+k^*+2k^*C_\mathrm{t}^*)k\rho T_0}, \tag{31}$$

which expresses the photophoretic velocity of the particle given by Eq. (1) in the limit $\lambda = 0$, and

$$G = \frac{1-k^*+k^*C_\mathrm{t}^*}{2+k^*+2k^*C_\mathrm{t}^*}. \tag{32}$$

It can be found that $-1 \le G \le 1/2$. For a large particle ($l/a \ll 1$) with $k^* \gg 1$, $G \to -1$, while for $k^* \ll 1$, $G \to 1/2$. Finally, when $k^* = (1-C_\mathrm{t}^*)^{-1}$, $G = 0$.

The normalized photophoretic velocity of the aerosol sphere, $U/U^{(0)}$, as calculated from Eq. (30), is plotted versus the separation parameter, λ, in Figs. 2 and 3 for various values of the parameters k^*, C_t^*, C_m^*, and $\hat{C}_\mathrm{m}^*$. Obviously, $U/U^{(0)}$ equals unity in the limit $\lambda = 0$ and decreases monotonically with increasing λ for any given values of k^*, C_t^*, C_m^*, and $\hat{C}_\mathrm{m}^*$. Fig. 2 illustrates the results of $U/U^{(0)}$ as a function of λ for the case of $C_\mathrm{t}^* = 2C_\mathrm{m}^*$ and $k^* = 100$ with C_m^* and $\hat{C}_\mathrm{m}^*$ as parameters. For the case of $\hat{C}_\mathrm{m}^* = \lambda C_\mathrm{m}^*$ (or $\hat{C}_\mathrm{m} = C_\mathrm{m}$), as displayed in Fig. 2(a), $U/U^{(0)}$ is not necessarily a monotonic function of the slip parameters C_m^* and $\hat{C}_\mathrm{m}^*$ for a fixed value of λ. However, for the case of $\hat{C}_\mathrm{m}^* = 0$, $U/U^{(0)}$ decreases monotonically with increasing C_m^* for a given value of λ, as illustrated in Fig. 2(b). Examining Eq. (30), reveals that this tendency between $U/U^{(0)}$ and C_m^* also exists for all *values of* k^* *other than 100.*

The sphere-in-cavity solution for a parallel problem concerning the sedimentation of an aerosol sphere was presented by Keh and Chang [20]. Different from the case of photophoresis, the normalized particle mobility predicted in the system of sedimentation increases monotonically with an increase in C_m^* for a constant value of λ. Also, the effect of the cavity wall on the photophoresis of the particle is much weaker than that on the sedimentation. The leading order of this boundary effect is λ^3 for photophoretic motion, compared with the effect of order λ for sedimentation. The reason for the weaker boundary effect on photophoresis is that the disturbance to the fluid velocity field caused by a photophoretic (or thermophoretic) particle decays faster (as r^{-3}) than that caused by an aerosol particle moving under the influence of a body force (as r^{-1}) [21].

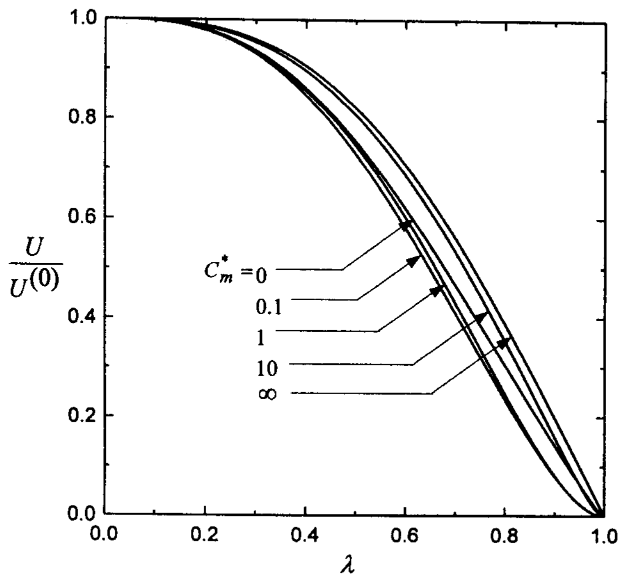

Fig. 2(a)

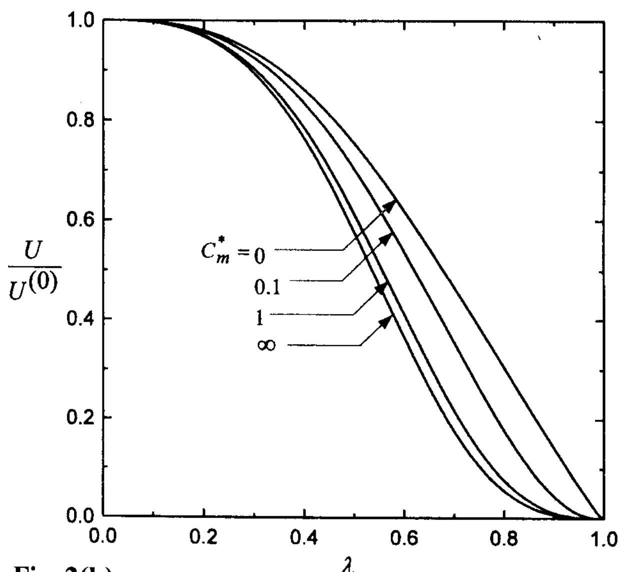

Fig. 2(b)

Fig. 2. Plots of the normalized photophoretic velocity for a spherical particle located at the center of a spherical cavity as a function of λ with $C_t^* = 2C_m^*$ and $k^* = 100$ with C_m^* as a parameter: (a) $\hat{C}_m^* = \lambda C_m^*$; (b) $\hat{C}_m^* = 0$.

The analytical results of $U/U^{(0)}$ as a function of λ for an aerosol sphere with $C_t^* = 2C_m^* = 0.2$ (a typical representative case) are plotted in Fig. 3, with k^* and $\hat{C}_m^*$ as parameters. For a given value of λ, $U/U^{(0)}$ increases monotonically with increasing k^*. This behavior is predictable, given that the temperature gradients on the particle surface near a wall with a constant temperature increase with the relative conductivity of the particle k^*. A comparison of Figs. 3(a) and 3(b) reveals that $U/U^{(0)}$ increases with increasing of $\hat{C}_m^*$ for constant values of k^* and λ. Examining Eq. (30) reveals that this trend of dependence of $U/U^{(0)}$ on k^* also exists for all values of C_t^* and C_m^*. Notably, a particle with a relatively high conductivity reduces the local temperature gradient (and thus, the thermal slip effect) along the particle surface, the photophoretic velocity of an isolated particle, $U^{(0)}$, is a monotonically decreasing function of k^* (and of C_t^* and C_m^*), as predicted by Eq. (31).

4. Concluding Remarks

The photophoresis of a spherical particle in a concentric spherical cavity filled with a gaseous medium has been analyzed herein. The surface properties, such as frictional slip coefficient, of the particle and cavity are allowed to differ. Based on the assumption of small Knudsen, Peclet, and Reynolds numbers, the temperature and fluid flow fields for this axisymmetric motion are analytically solved and the particle velocity is obtained in the closed-form expression (30). This photophoretic velocity decreases monotonically relative to its undisturbed value with increasing ratio of particle-to-cavity radii λ and with decreasing relative conductivity k^* of the particle. The analytical results demonstrate that the boundary effect of the cavity wall on the photophoretic motion of an aerosol particle can be significant in certain circumstances. In practical aerosol systems, the boundary effect of a particle on photophoresis is obviously weaker than that on

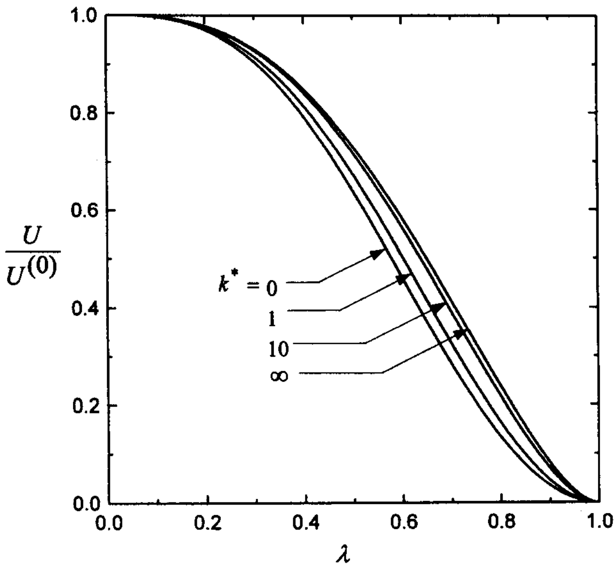

Fig. 3(a)

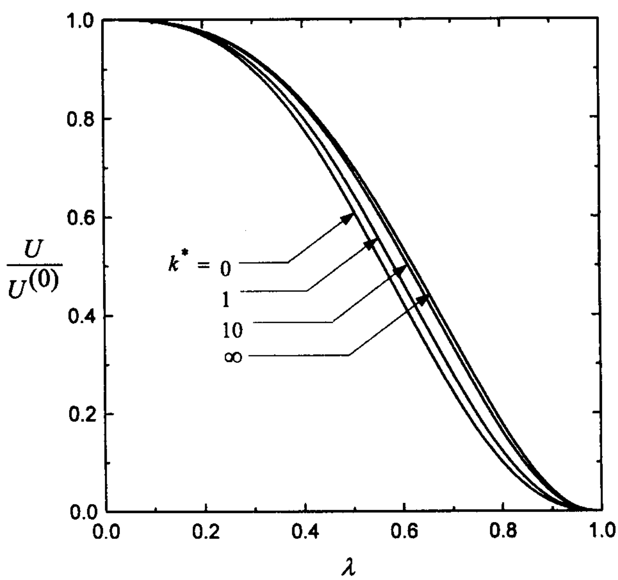

Fig. 3(b)

Fig. 3 Plots of the normalized photophoretic velocity for a spherical particle located at the center of a spherical cavity as a function of λ with $C_t^* = 2C_m^* = 0.2$ with k^* as a parameter: (a) $\hat{C}_m^* = \lambda C_m^*$; (b) $\hat{C}_m^* = 0$.

the particle motion driven by gravity.

As mentioned earlier, Eq. (30) is obtained based on continuum model for the gas phase with a slip-flow boundary condition on the particle surface. For a perfect gas, the kinetic theory predicts that the mean free path of the gasmolecules is inversely proportional to the pressure [22]. For example, the mean free path of air molecules at 25 °C is approximately 67 nm at 1 atm and is around 51 μm at 1 torr. Therefore, the results obtained herein with assuming a small Knudsen number can be used for a broad range of particle sizes close to atmospheric pressure, but are only applicable for relatively large particles at low pressures.

Acknowledgements

The author would like to thank the National Science Council of the Republic of China for partially supporting this research. Mr. Y. S. Chen is appreciated for his assistance with some of the mathematical work.

Nomenclature

a = particle radius (m)

A_n, B_n = coefficients in Eqs. (8) and (9)

b = radius of the cavity (m)

$B(\zeta,\theta)$ = dimensionless electric field distribution function defined by Eq. (4)

C, D, E, F = coefficients in Eq. (20) (m^4s^{-1}, m^2s^{-1}, $m\,s^{-1}$, $m^{-1}s^{-1}$)

$C_m, \hat{C}_m$ = dimensionless coefficients accounting for the frictional slip on the particle surface and cavity wall, respectively

C_m^*, $\hat{C}_m^*$ = $C_m l/a$ and $\hat{C}_m l/a$, respectively

C_s = dimensionless coefficient accounting for the thermal slip on the particle surface

C_t = dimensionless coefficient accounting for the temperature jump on the particle surface

$C_t^* = C_t l/a$

G = parameter defined by Eq. (32)

I = intensity of the incident light beam ($W\,m^{-2}$)

J_1 = the photophoretic asymmetry factor of the particle defined by Eq. (26)

k = thermal conductivity of the fluid ($W\,m^{-1}K^{-1}$)

k_p = thermal conductivity of the particle

$(\mathrm{W\,m^{-1}K^{-1}})$

$k^* = k_p / k$

l = mean free path of the gas molecules (m)

r = radial spherical coordinate (m)

$S_n(\zeta)$ = function of ζ defined by Eq. (10)

T = temperature distribution in the fluid phase (K)

T_p = temperature distribution inside the particle (K)

T_0 = temperature of the cavity wall (K)

U = photophoretic velocity of a particle $(\mathrm{m\,s^{-1}})$

$U^{(0)}$ = photophoretic velocity of an isolated particle $(\mathrm{m\,s^{-1}})$

v_r, v_θ, v_ϕ = components of the fluid velocity in spherical coordinates $(\mathrm{m\,s^{-1}})$

V = characteristic velocity defined by Eq. (23) $(\mathrm{m\,s^{-1}})$

z = coordinate in the direction of incident light (m)

Greek Letters

$\zeta = r / a$

η = viscosity of the fluid $(\mathrm{kg\,m^{-1}s^{-1}})$

θ, ϕ = angular spherical coordinates

$\lambda = a / b$

λ_0 = the wavelength of the incident light beam (m)

υ, κ = real and imaginary parts of the complex refractive index of the particle

ρ = density of the fluid $(\mathrm{kg\,m^{-3}})$

Ψ = Stokes stream function of the fluid flow $(\mathrm{m^3s^{-1}})$

References

1. Orr C. and Keng E. Y. H. (1964), Photophoretic effects in the stratosphere. J. Atmos. Sci. 21: 475.
2. Preining O., Photophoresis, in Davies C. N. (Ed.) (1966), Aerosol Science, Academic Press, New York, p. 111.
3. Kennard E. H. (1938), Kinetic Theory of Gases, McGraw-Hill, New York, p. 291.
4. Arnold S. and Lewittes M. J. (1982), Size dependence of the photophoretic force. Appl. Phys. 53: 5314.
5. Chernyak V. and Beresnev S. J. (1993), Photophoresis of aerosol particles. J. Aerosol Sci. 24: 857.
6. Kerker M. and Cooke D. D. J. (1982), Photophoretic force on aerosol particles in the free-molecule regime. Opt. Soc. Am. 72: 1267.
7. Mackowski D. W. (1989), Photophoresis of aerosol particles in the free molecular and slip-flow regimes. Int. J. Heat Mass Transfer 32: 843.
8. Reed L. D., (1977), Low Knudsen number photophoresis. J. Aerosol Sci. 8: 123.
9. Yalamov Yu. I., Kutukov V. B. and Shchukin E. R. (1976), Theory of the photophoretic motion of the large-size volatile aerosol particle. J. Colloid Interface Sci. 57: 564.
10. Talbot L., Cheng R. K., Schefer R. W. and Willis D. R. (1980), Thermophoresis of particles in a heated boundary layer. J. Fluid Mech. 101: 737.
11. Keh H. J. and Tu H. (2001), Thermophoresis and photophoresis of cylindrical particles. J. Colloids Surfaces A, 176: 213.
12. Giddings J. C., Kucera E., Russell C. P. and Myers M. N. (1968), Statistical theory for the equilibrium distribution of rigid molecules in inert porous networks. Exclusion chromatography. J. Phys. Chem. 72: 4397.
13. Glandt E. D. (1981), Distribution equilibrium between a bulk phase and small pores. AIChE J. 27: 51.
14. Bungay P. M. and Brenner H. (1973), The motion of a closely-fitting sphere in a

fluid-filled tube. Int. J. Multiphase Flow 1: 25.

15. Happel J. and Brenner H. (1983), Low Reynolds Number Hydrodynamics, Martinus Nijhoff, The Netherlands.
16. Zydney A. L. (1995), Boundary effects on the electrophoretic motion of a charged particle in a spherical cavity. J. Colloid Interface Sci. 169: 476.
17. Keh H. J. and Chiou J. Y. (1996), Electrophoresis of a colloidal sphere in a circular cylindrical pore. AIChE J. 42: 1397.
18. Greene W. M., Spjut R. E., Bar-Ziv E., Sarofim A. F. and Longwell J. P. (1985), Photophoresis of irradiated spheres: absorption centers. J. Opt. Soc. Am. B, 2: 998.
19. Brock J. R. (1962), On the theory of thermal forces acting on aerosol particles. J. Colloid Sci. 17: 768.
20. Keh H. J. and Chang J. H. (1998), Boundary effects on the creeping-flow and thermophoretic motions of an aerosol particle in a spherical cavity. Chem. Eng. Sci. 53: 2365.
21. Keh H. J. and Chen S. H. (1995), Particle interactions in thermophoresis. Chem. Eng. Sci. 50: 3395.
22. Shoemaker D. P., Garland C. W., Steinfeld J. I. and Nibler J. W. (1981), Experiments in Physical Chemistry, Fourth ed., McGraw-Hill, New York.

Received for review, April 19, 2001
Accepted, May 8, 2001
AAQR-2001-03